

## Guest–Host Interactions in As-Made Al-ZSM-12: Implications for the Synthesis of Zeolite Catalysts

Daniel F. Shantz,<sup>§</sup> Christian Fild,<sup>†</sup> Hubert Koller,<sup>†</sup> and Raul F. Lobo<sup>\*,§</sup>

*Institut für Physikalische Chemie, Westfälische-Wilhelms Universität Münster, Schlossplatz 417, D-48149 Münster, Germany, and Center for Catalytic Science and Technology, Department of Chemical Engineering, University of Delaware, Newark Delaware 19716*

*Received: July 23, 1999; In Final Form: September 30, 1999*

Al-ZSM-12 samples have been prepared with selectively deuterated benzyltrimethylammonium cations as structure-directing agents (SDAs) to study the motion of the SDA and the spatial relationships between the SDA and the zeolite framework. <sup>2</sup>H NMR shows the methyl groups of the structure-directing agent undergo at least two rapid rotations while the benzyl segment is essentially immobile, undergoing only small angle wobbling motions. Cross-polarization and rotational echo double resonance NMR experiments were performed to study the spatial relationships between the SDA and the framework silicon and aluminum. The results from the CPMAS and REDOR experiments show the methylene protons of the structure-directing agent are preferentially located near the silicon atoms adjacent to the framework aluminum. As a consequence there is relative charge ordering between the SDA and the framework aluminum, suggesting that the framework aluminum is directly associated with the charge center of the SDA. Given the reduced number of configurations accessible to the SDAs in the as-made material, we believe the results suggest a possible route to tailoring the spatial arrangement of trivalent framework atoms through selection of SDAs with appropriate charge distributions.

### Introduction

Zeolites are an important class of microporous solids that are used in heterogeneous catalysis, adsorption and separation of gases, and ion-exchange operations.<sup>1</sup> There is interest not only in the synthesis of new zeolites with novel framework topologies<sup>2</sup> but also in understanding how to tailor the catalytic and adsorptive properties of existing materials.<sup>3</sup> Postsynthetic procedures such as ion exchange, acid treatment, and vapor phase impregnation have been used to modify physical properties such as acidity and adsorption selectivity and to introduce bifunctionality into zeolites.<sup>4</sup> Another approach is to modify physical properties directly through altering the synthesis conditions. However, the mechanisms of zeolite synthesis and structure direction are not well enough understood to make such an approach generally feasible. For example, the ability to alter the spatial distribution of trivalent atoms such as Al<sup>3+</sup> in the zeolite framework during synthesis could allow control over the relative rates of hydride transfer versus cracking in hydrocarbon conversions. Certain steps in reaction pathways may be favored if two active sites are close together instead of being isolated, leading to different product distributions.

One possible route to tailoring the physical properties of zeolites through synthesis would be to exploit different interactions in the synthesis gel between the organic structure-directing agent (SDA) and the silicate species. With this in mind, we have studied as-made all-silica zeolites and demonstrated the presence of strong Coulombic forces between cationic structure-directing agents and charge-compensating defect sites.<sup>5</sup> Both

<sup>2</sup>H NMR and multidimensional NMR spectroscopy results of several as-made all-silica zeolites are consistent with the presence of charge ordering. The study reported here was undertaken to determine whether similar Coulombic forces exist between cationic SDAs and aluminum in the framework of zeolites.

Samples of as-made Al-ZSM-12 (Si/Al = 28) synthesized with selectively deuterated benzyltrimethylammonium cations were studied using multinuclear NMR spectroscopy. NMR was chosen to study these materials because it is sensitive to structural features at short lengths scales ( $\leq 1$  nm). Further, the structural feature of interest does not need to exhibit long-range ordering and typically SDAs and trivalent framework atoms are not ordered in the crystallographic sense.<sup>6</sup> ZSM-12 (MTW) is a large-pore zeolite with a one-dimensional elliptical pore architecture with dimensions of approximately  $5.5 \times 5.9 \text{ \AA}^7$  and can be synthesized with or without aluminum in the synthesis gel. The Si/Al ratio of the samples studied here was adjusted so that the organic SDA to aluminum ratio is approximately 1.

The dynamics of the SDAs were characterized using <sup>2</sup>H NMR, a technique sensitive to molecular motions with  $10^3 < \tau_c < 10^8 \text{ s}^{-1}$ .<sup>8</sup> Cross-polarization magic angle spinning (CPMAS)<sup>9</sup> and rotational echo double resonance (REDOR)<sup>10</sup> NMR experiments were used to study the relative orientation and spatial proximity of the SDA with respect to the zeolite framework. The strong spatial dependence on the rate of cross-polarization ( $\propto 1/r^6$ ) makes CPMAS experiments a useful qualitative tool for studying solids. REDOR experiments also rely on dipolar coupling ( $\propto 1/r^3$ ) to study structural features in solids.<sup>10</sup> The REDOR and CPMAS pulse sequences are shown in Figure 1. The REDOR experiment is performed as a difference experiment. The first spectrum is acquired using a

\* Corresponding author Phone: (302) 831-1261. Fax: (302) 831-2085. E-mail: lobo@che.udel.edu.

<sup>†</sup> Westfälische-Wilhelms Universität Münster.

<sup>§</sup> University of Delaware.

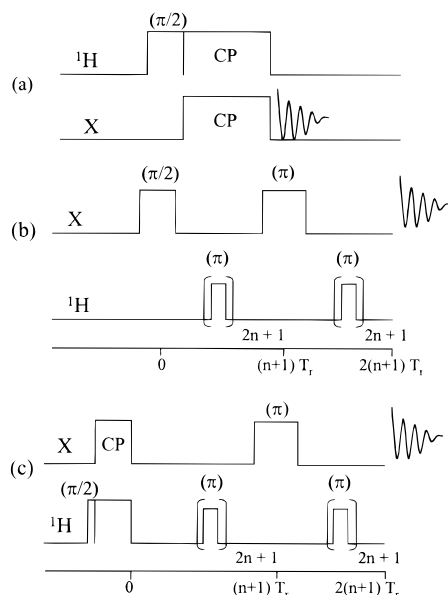


**Figure 1.** Pulse sequences used for (a) cross-polarization magic-angle spinning (CPMAS), (b) rotational echo double resonance (REDOR), and (c) CP-REDOR experiments. In (b) and (c) the third line shows the rotor cycle, where  $n = 0, 1, 2, \dots$  and  $T_r$  is the rotor period.

spin echo pulse sequence where the nucleus of interest (i.e.,  $^{29}\text{Si}$ ) is observed. A second spectrum (REDOR spectrum) is then acquired with a spin echo pulse sequence applied to the observed nucleus while additional rotor-synchronized  $180^\circ$  pulses (called dephasing pulses) are applied to the coupled nucleus (i.e.,  $^1\text{H}$ ) during the evolution time of the spin echo. The rotor-synchronized  $180^\circ$  pulses reintroduce the weak dipolar coupling that is eliminated by magic-angle spinning. The heteronuclear dipolar coupling between nuclei leads to incomplete refocusing of the spin echo in the presence of the dephasing pulses. The extent to which the spin echo signal is attenuated in the presence of the dephasing pulses is related to the strength of the dipolar coupling between the spins. The delay time between the  $90^\circ$  and  $180^\circ$  pulses of the spin echo is then increased, resulting in more dephasing pulses being applied to the coupled nucleus as the evolution period is increased. In this way the REDOR signal intensity can be studied as a function of the evolution time. The REDOR fraction ( $\Delta S = (S_0 - S)/S_0$ ), which is the normalized intensity difference between the REDOR ( $S$ ) and spin echo ( $S_0$ ) spectra, is plotted as a function of the evolution time, generating a REDOR curve. The stronger the dipolar interaction between the coupled nuclei (i.e., the closer they are to each other), the faster the REDOR signal decays and the steeper the initial slope of the REDOR curve. In the limiting case of isolated and rigid spin pairs, REDOR can be used to obtain quantitative internuclear distances.<sup>10</sup> Due to the complexity of the materials studied here quantitative distances cannot be determined, but by performing CPMAS and REDOR experiments on samples with different selectively deuterated SDAs several conclusions can be drawn about the relative orientation and proximity of the SDA with respect to the zeolite framework.

$^2\text{H}$  NMR results show the methyl groups of the SDA undergo at least two rapid rotations, whereas the benzyl group is essentially immobile on the  $^2\text{H}$  NMR time scale.  $^{27}\text{Al}\{^1\text{H}\}$  REDOR results indicate that the aluminum is in close proximity to the structure-directing agent.  $^{29}\text{Si}\{^1\text{H}\}$  CPMAS and CP-REDOR show that the methylene protons of the SDA are preferentially ordered near framework silicon atoms adjacent to aluminum. The CPMAS and REDOR results imply the charge

of the SDA is in close spatial proximity to the framework aluminum. These results are consistent with the presence of Coulombic forces between the cationic SDA and framework aluminum and show that the aluminum in the framework is directly associated with the charge center of the organic SDA. Further, we believe the results indicate that with (i) basic knowledge of the geometric arrangement of the SDAs in the zeolite micropores and (ii) selecting SDAs with different charge distributions, it should be possible to alter the spatial arrangement of trivalent atoms in the zeolite framework.

## Experimental Section

**Zeolite Synthesis.** Samples of Al-ZSM-12 were synthesized using a stoichiometry of  $1 \text{ SiO}_2 \cdot 0.022 \text{ Al}_2\text{O}_3 \cdot 0.175 \text{ NaOH} \cdot 0.135 \text{ R}^+\text{OH}^- \cdot 38 \text{ H}_2\text{O}$ , where  $\text{R}^+\text{OH}^-$  is benzyltrimethylammonium hydroxide. Benzyltrimethylammonium hydroxide was prepared as follows: 4 mL of benzyl chloride (98% Fluka) were added to 100 mL of acetone (99+% ACS Reagent, Aldrich), followed by the addition of 11 mL of trimethylamine (TMA) (4.2 M in ethanol, Fluka). This solution was allowed to react overnight in the absence of light, and then the solvent and other volatiles were removed under vacuum at  $50\text{--}60^\circ\text{C}$  in a rotavapor (yield  $\geq 95\%$ ). The resulting solids were collected by filtration, washed with 100 mL of ethyl ether (99+% anhydrous, Fisher) and allowed to dry. The chloride salt was converted to the hydroxide form using a 5-fold excess of ion-exchange resin (IONAC NA-38,  $\text{OH}^-$  form). The conversion of the chloride to hydroxide is greater than 95% based on titration of the resultant solution. The  $^{13}\text{C}$  NMR chemical shifts for the chloride salt in  $\text{D}_2\text{O}$  are  $\delta = 135.2, 133.2, 131.6, 129.8, 71.7, \text{ and } 54.5$  ppm.

A typical synthesis for Al-ZSM-12 is as follows: 3 g of Cab-O-Sil (M5 grade) was added to 25 mL of a 0.3 N solution of benzyltrimethylammonium hydroxide. A 0.40 g amount of NaY (Si/Al = 2.4, Zeolyst) was added to this solution while mixing, and 7 mL of deionized water was then added followed by the addition of 0.30 g of ground NaOH (95+% Aldrich). The resulting gel was mixed for approximately 2 h. The solution was then sealed in two 23 mL Teflon-lined Parr autoclaves and heated at  $160^\circ\text{C}$  for 7 days under autogenous pressure with sample rotation ( $\sim 30$  rpm). After the synthesis period the autoclaves were cooled and the solids were collected by filtration, washed several times with deionized water, and dried overnight at  $80^\circ\text{C}$ .

Samples were also made with selectively deuterated organics. Structure-directing agents deuterated at the methylene ( $d_2$ ), aromatic ring ( $d_5$ ), and both ring and methylene ( $d_7$ ) positions were synthesized as described above using the suitably labeled benzyl chloride (98%+D, Isotec). Methyl-labeled ( $d_9$ ) and methyl- and ring-labeled ( $d_{14}$ ) structure-directing agents were also prepared in a similar manner using a solution of  $d_9$ -TMA in ethanol. The  $d_9$ -TMA solution was prepared by slowly bubbling  $d_9$ -TMA (98%+D Cambridge Isotopes) gas into a solution of ethanol immersed in an ice bath. The rest of the synthesis was carried out as described above. Complete selective deuteration was verified by  $^1\text{H}$  solution NMR (not shown). The deuterated SDAs used are shown in Figure 2.

**Analytical Details.** Powder X-ray diffraction (XRD) was performed using a Phillips 3000 X'Pert System with  $\text{Cu K}\alpha$  radiation. The patterns used for indexing were collected from  $4\text{--}50^\circ 2\theta$  using the step scan mode, a  $0.02^\circ$  step size, and 15 s count time per step. The peak deconvolution was carried out using the Phillips package ProFit, and refinement of the unit cell parameters was done with the program Lapod.<sup>11</sup> TGA measurements were performed with a Cahn TG-121 microbal-

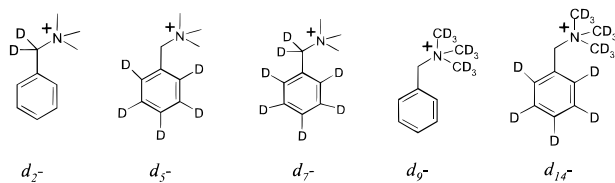


**Figure 2.** Selectively deuterated benzyltrimethylammonium cations used in synthesis.

ance with a heating rate of 2 °C/min from room temperature to 650 °C. Elemental analysis for Si, Al, and Na was performed by Galbraith Laboratories (Knoxville, TN).

Solution  $^{13}\text{C}$  and  $^1\text{H}$  NMR spectra were measured using a Bruker AC 250 spectrometer operating at 62.26 and 250 MHz with the chemical shifts referenced to tetramethylsilane.  $^{29}\text{Si}$ ,  $^{13}\text{C}$ ,  $^{27}\text{Al}$ ,  $^1\text{H}$ , and  $^2\text{H}$  solid-state NMR spectra were measured on a Bruker MSL 300 spectrometer at 59.63, 75.47, 78.25, 300.13, and 46.07 MHz, respectively. Chemical shifts for the  $^{29}\text{Si}$ ,  $^{13}\text{C}$ , and  $^1\text{H}$  spectra are referenced to tetramethylsilane. Chemical shifts quoted for  $^{27}\text{Al}$  spectra are referenced to aqueous 1.0 M  $\text{Al}(\text{NO}_3)_3$ . The structural integrity of the structure-directing agents inside the as-made samples was verified by  $^{13}\text{C}$  CPMAS NMR using a contact time of 5 ms, a spinning rate of 3 kHz, a  $90^\circ$   $^1\text{H}$  pulse of 6  $\mu\text{s}$ , and high-power proton decoupling. One-pulse  $^{29}\text{Si}$  MAS NMR spectra were acquired using a 7 mm probe with  $\text{ZrO}_2$  rotors, a spinning rate of 3 kHz, a 4  $\mu\text{s}$   $60^\circ$  pulse, high-power proton decoupling, and a 60 s recycle delay to avoid relaxation effects in the signal intensities.  $^{29}\text{Si}\{^1\text{H}\}$  CPMAS spectra were acquired using a 6  $\mu\text{s}$   $^1\text{H}$   $90^\circ$  pulse, a spinning rate of 3 kHz, a recycle delay of 5 s, and high-power proton decoupling, and the Hartmann–Hahn match was optimized on a sample of Al-ZSM-12 made with a fully protonated SDA.  $^1\text{H}$  MAS spectra were acquired using a 4 mm probe with  $\text{ZrO}_2$  rotors, a spinning rate of 10 kHz, a 5 s recycle delay, and a 5  $\mu\text{s}$   $90^\circ$  pulse.  $^1\text{H}$  spin–lattice ( $T_1$ ) relaxation experiments were performed to determine the recycle delay necessary for complete relaxation of all protons.  $^{27}\text{Al}$  MAS spectra were acquired using a 4 mm probe with  $\text{ZrO}_2$  rotors, a spinning rate of 10 kHz, a 2 s recycle delay, and 1  $\mu\text{s}$   $\pi/12$  pulses. Static  $^2\text{H}$  spectra were acquired using the quadrupole echo pulse sequence with a 3  $\mu\text{s}$   $90^\circ$  pulse, 30  $\mu\text{s}$  echo delay, and 3 s recycle delay.  $^2\text{H}$  MAS spectra were acquired using a rotor-synchronized quadrupole echo sequence with a 100  $\mu\text{s}$  echo interval, a spinning rate of 10 kHz, a 4  $\mu\text{s}$   $90^\circ$  pulse, and a 3 s recycle delay.  $^{29}\text{Si}$ ,  $^1\text{H}$ , and  $^2\text{H}$  MAS NMR line shape simulations were performed using NUTS from Acorn NMR.

$^{27}\text{Al}\{^1\text{H}\}$  REDOR experiments were performed on a Bruker Avance DSX 500 spectrometer operating at 130.32 and 500.13 MHz for  $^{27}\text{Al}$  and  $^1\text{H}$ , respectively. A total of 320 scans were acquired for each spectrum using a 16 step phase cycling routine, the spinning rate was 10 kHz, a 2 s recycle delay was used, and 32 REDOR points were collected for each sample. The lengths of the pulses were optimized for each sample, with typical values of 4.25, 7.75, and 11.5  $\mu\text{s}$  for the  $^{27}\text{Al}$   $90^\circ$  and  $180^\circ$  and  $^1\text{H}$   $180^\circ$  pulses, respectively. All samples were dried under vacuum at 100 °C overnight and packed into rotors immediately before use to eliminate the presence of water.

$^{29}\text{Si}\{^1\text{H}\}$  CP-REDOR experiments were performed on a MSL 300 spectrometer using a 5 s recycle delay, a 6  $\mu\text{s}$   $^1\text{H}$   $90^\circ$  pulse length, and a contact time of 10 ms. The spinning rate was 3 kHz and a 32 step phase cycling routine was used. The Hartmann–Hahn match and the  $^{29}\text{Si}$  and  $^1\text{H}$   $180^\circ$  pulse lengths were optimized on the sample of Al-ZSM-12 made with a fully protonated SDA. Typical pulse lengths were 12.1 and 12.0  $\mu\text{s}$

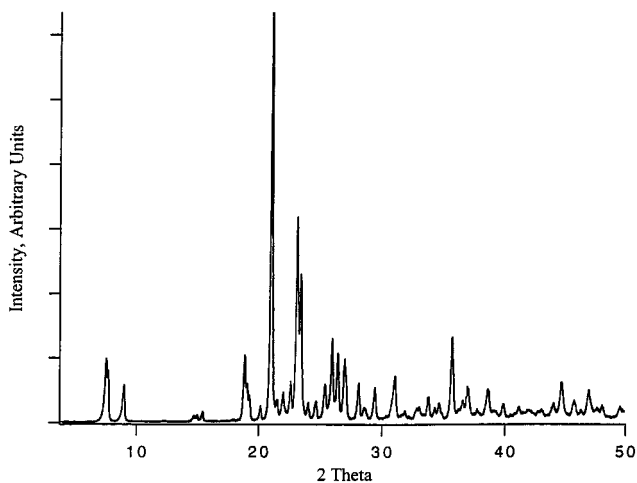


**Figure 3.** Powder X-ray diffraction pattern of as-made Al-ZSM-12.

for the  $^{29}\text{Si}$  and  $^1\text{H}$   $180^\circ$  pulses, respectively. The number of scans per spectrum is sample dependent and is indicated in the figures. The number of points acquired involves a tradeoff between the necessary signal-to-noise and the acquisition time. For example, the acquisition of four REDOR points for the  $d_{14}$ -ZSM-12 sample took approximately 50 h. All samples used for the  $^{29}\text{Si}$  CP-REDOR experiments were dried at 100 °C for at least 18 h prior to the experiments and were packed into rotors immediately after the heating period to eliminate the presence of water.

## Results

**Material Characterization.** The X-ray diffraction (XRD) pattern of as-made Al-ZSM-12 is shown in Figure 3. On the basis of the indexed XRD patterns all materials are crystalline and contain no amorphous impurities. The unit cell parameters of the as-made material are  $a = 24.937 \text{ \AA}$ ,  $b = 5.020 \text{ \AA}$ ,  $c = 24.333 \text{ \AA}$ , and  $\beta = 107.71^\circ$ .<sup>7b</sup> The XRD patterns of samples made with labeled SDAs were also indexed, and the results are essentially identical to the values above in all cases. TGA experiments performed on the as-made material indicate a weight loss of 8.2% above 200 °C, corresponding to 2.0 SDAs per unit cell. There are four channels per unit cell of ZSM-12; however, the benzyltrimethylammonium cations span two unit cells in the  $b$  direction.

The  $^{29}\text{Si}$  one-pulse NMR spectrum of as-made Al-ZSM-12 is shown in Figure 4. The spectrum contains three components, one due to silicon atoms with one aluminum atom in the second coordination sphere (Si1Al), and two due to silicon atoms with no aluminum atoms in the second coordination sphere (Si0Al).<sup>12</sup> Three lines are used to deconvolute the spectrum, one for the (Si1Al) component ( $\delta = -104.5$  ppm) and two for the (Si0Al) components ( $\delta = -110.1$ ,  $-113.8$  ppm). The Si/Al ratio determined from  $^{29}\text{Si}$  NMR is approximately 28, in excellent agreement with elemental analysis (Si/Al = 28.0, 2 Al per unit cell). The resonance at  $-104.5$  ppm is not due to silanol  $\text{Q}^3$  groups (where  $\text{Q}^n$  stands for  $\text{X}_{4-n}\text{Si}[\text{OSi}]_n$ ,  $\text{X} = \text{OH}$  or  $\text{O}^-$ )<sup>12</sup> in the zeolite framework on the basis of the following evidence.  $^{29}\text{Si}$  CPMAS NMR using a short (1 ms) contact time shows no enhancement of the resonance at  $-104.5$  ppm, which would be observed if the resonance was due to silanol  $\text{Q}^3$  groups. Also,  $^{29}\text{Si}$  NMR of the calcined material shows no appreciable changes as compared to the as-made material. Finally, the  $\text{Q}^3$  resonance for all-silica ZSM-12 made with the same SDA is observed at a chemical shift value of  $-102.5$  ppm (not shown). There is only one resonance in  $^{27}\text{Al}$  NMR spectra of the as-made samples

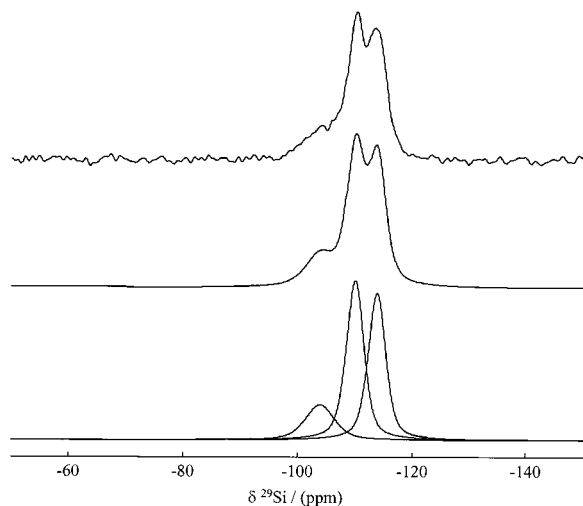


Figure 4. One-pulse  $^{29}\text{Si}$  NMR spectrum of as-made Al-ZSM-12.

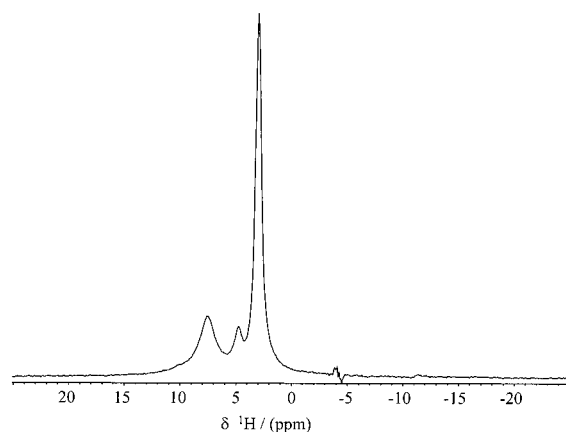


Figure 5.  $^1\text{H}$  NMR spectrum of as-made Al-ZSM-12 synthesized with a fully protonated SDA.

at 56 ppm due to aluminum in a tetrahedral environment.  $^{13}\text{C}\{-^1\text{H}\}$  CPMAS experiments (not shown) verify the SDAs are intact in the as-made materials within the detection limits of NMR.

The  $^1\text{H}$  NMR spectrum of Al-ZSM-12 made with a fully protonated SDA before dehydration is shown in Figure 5. There is a line at 3.1 ppm due to the methyl protons, a broad asymmetric line at 4.4 ppm due to the methylene protons, and a broad resonance at 7.4 ppm due to the aromatic protons. There is no resonance at 10.5 ppm due to silanol groups in the zeolite framework associated with charge-compensating defect sites that are common in fully siliceous as-made zeolites.<sup>13</sup> This is consistent with the  $^{29}\text{Si}$  NMR results that show there are very few or no  $\text{Q}^3$  groups present. Also,  $^1\text{H}$  NMR on samples with selectively deuterated SDAs are consistent with this interpretation. A resonance at 10.4 ppm is only observed for the  $d_{14}$  sample, and it is approximately 3.6% of the total integrated intensity. There are two important consequences of these materials containing very few/no defect silanols. First, in the case of the  $^{27}\text{Al}\{^1\text{H}\}$  REDOR experiments there are only organic protons present. Second, the dephasing observed of the (Si1Al) resonance in the  $^{29}\text{Si}\{^1\text{H}\}$  CP-REDOR experiments is due to dipolar interactions with the SDA and not a result of silanol protons.

**Molecular Motion of the SDA.** The static deuterium NMR spectrum of the methyl ( $d_9$ ) labeled sample is shown in Figure 6. The line shape suggests the methyl groups' motion consists of multiple rotations. There are two components in the line

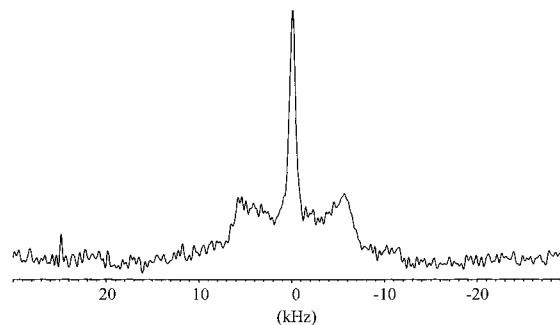
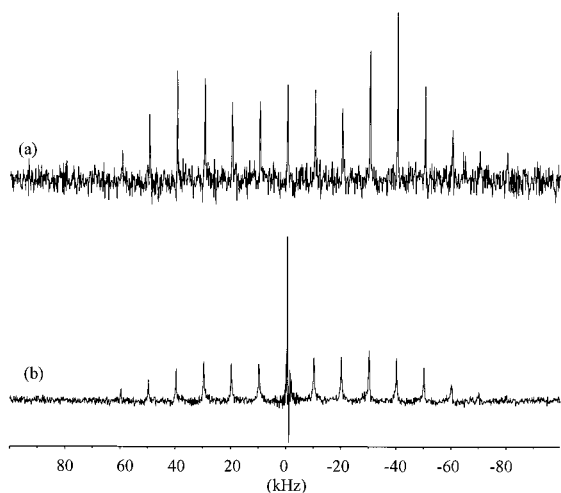


Figure 6. Static  $^2\text{H}$  NMR spectrum of as-made Al-ZSM-12 synthesized with an SDA labeled at the methyl ( $d_9$ ) position.

shape, one that has a quadrupole coupling constant (QCC) of 15.9 kHz and asymmetry parameter  $\eta = 0.03$ , and another component that is a narrow Lorentzian line (fwhm = 685 Hz). The broad (15.9 kHz) component (77% of the integrated spectral intensity) is due to deuterons undergoing two rotations, a rotation about the methyl groups'  $C_3$  axes and a rotation about the nitrogen's  $C_3$  axis. There is an additional motion, likely librational in nature, which accounts for the QCC being less than would be expected for just the two rotations (QCC = 19 kHz) and the nonzero asymmetry parameter. The narrow component might be attributed to SDAs undergoing isotropic reorientation; however, this is inconsistent with  $^2\text{H}$  NMR results for the samples deuterated at the methylene and aromatic positions (vide infra). Experiments were also performed on the methyl-labeled sample where the delay  $\tau$  between the pulses of the quadrupole echo was varied. Variable echo delay experiments can be used to discern if motion rates are in the intermediate regime ( $\tau_c \sim 10^6 \text{ s}^{-1}$ ).<sup>14</sup> The results from those experiments show that neither motion is in the intermediate motion regime at room temperature.  $^2\text{H}$  spin–lattice ( $T_1$ ) relaxation experiments show that the narrow component has a larger  $T_1$  value than the broad component. One possibility could be that the narrow component is due to organic degradation products, but there are no degradation products observed for the fully protonated sample within the detection limits of  $^{13}\text{C}$  NMR.  $^2\text{H}$  NMR was also performed on a sample outgassed under vacuum for 8 h at room temperature, with no observed difference in the line shape. Finally, proton–deuteron exchange between the organic SDA and water and/or the silicate species in the synthesis mixture should not be a problem and has not been observed in any other of these samples or in any of our previous studies.<sup>5</sup> The cause of the narrow component present in the line shape is not known at this time.

$^2\text{H}$  MAS echo experiments were performed on the  $d_2$  (methylene) and  $d_5$  (aromatic) labeled samples (Figure 7). Quantitative analysis of the spectra is not warranted due to limitations with the spectrometer's hardware. The quadrupole coupling constants (QCCs) are approximately 110 and 100 kHz for the  $d_2$  and  $d_5$  samples, respectively. These values are consistent with essentially immobile deuterons, where likely the QCCs are less than the value expected for rigid deuterons due to small angle wobbling motions. Clearly, these segments of the SDA do not undergo isotropic reorientation on the NMR time scale. Static  $^2\text{H}$  NMR experiments performed on these samples (not shown) do not exhibit a Lorentzian component, consistent with the absence of isotropic motion. Also, the aromatic and methylene resonances in the  $^1\text{H}$  NMR spectrum of the  $d_9$  sample (not shown) have strong spinning sidebands, which indicate that the proton–proton dipolar coupling is not being averaged by molecular motion.



**Figure 7.**  $^2\text{H}$  MAS quadrupole echo spectra of as-made Al-ZSM-12 synthesized with (a) methylene labeled ( $d_2$ ) and (b) aromatic labeled ( $d_5$ ) SDAs.

On the basis of the deuterium NMR results the trimethylammonium segment of the SDA has a much higher degree of mobility than the benzyl group, undergoing at least two rapid rotations, and another small-angle wobbling or librational motion. The  $^2\text{H}$  MAS experiments show the restricted mobility of the benzyl group.

**Guest–Host Interactions.** The spatial relationships between the SDA and the zeolite framework were studied with CPMAS and REDOR experiments. CPMAS is an experimentally straightforward technique, though quantitative analysis of the data is usually not possible. On the other hand, REDOR experiments are much more demanding in terms of spectrometer capabilities and setup, but under favorable conditions quantitative results can be obtained. Quantitative analysis of the data (i.e., extraction of internuclear distances) is not warranted for the systems under consideration here, due to the segmental dependence of the SDA's mobility, the presence of nonisolated spin pairs, and disorder (both static and dynamic) of the SDA. However, clear trends can be discerned from the CPMAS and REDOR experiments.

$^1\text{H}\{^{27}\text{Al}\}$  REDOR observing the protons were the first experiments performed. Both the methylene ( $d_2$ ) and methyl ( $d_9$ ) labeled samples were studied since each of these samples have two resonances that are easily resolved in the  $^1\text{H}$  NMR. However, the aromatic protons have a small transverse ( $T_2$ ) relaxation time constant and as a result the spin echo signal decayed before a substantial REDOR effect could be observed. Consequently, the  $^1\text{H}\{^{27}\text{Al}\}$  REDOR experiments yielded no useful information, and other double-resonance experiments where the protons are observed (i.e., TRAPDOR) were not performed.

**CPMAS NMR.**  $^{29}\text{Si}\{^1\text{H}\}$  CPMAS spectra of Al-ZSM-12 samples acquired with a  $400\ \mu\text{s}$  contact time are shown in Figure 8. Selective enhancement of the (Si1Al) resonance is not observed for samples with deuterated benzyl ( $d_7$ ) and methyl ( $d_9$ ) groups. The (Si1Al)/(Si0Al) ratio for the fully protonated,  $d_7$ , and  $d_9$  samples are 0.32, 0.28, and 0.30, respectively. As a comparison, the (Si1Al)/(Si0Al) ratio for the one-pulse  $^{29}\text{Si}$  spectrum is 0.17. The (Si1Al) resonance is substantially enhanced when only the methylene protons are not labeled ( $d_{14}$ ) ((Si1Al)/(Si0Al) = 0.98). This is consistent with the methylene protons being preferentially ordered near silicon atoms adjacent to the framework aluminum. Despite the complex spin dynamics of the cross-polarization process, the  $d_{14}$  sample is close to an

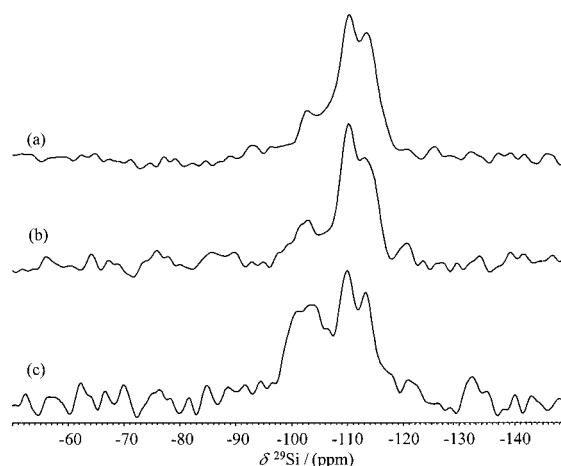


**Figure 8.**  $^{29}\text{Si}\{^1\text{H}\}$  CPMAS spectra of as-made Al-ZSM-12 with (a) benzyl-labeled ( $d_7$ ), (b) methyl-labeled ( $d_9$ ), and (c) aromatic- and methyl-labeled ( $d_{14}$ ) SDAs. A contact time of  $400\ \mu\text{s}$  was used and 5733, 5125, and 7774 scans were acquired for (a), (b), and (c), respectively.

ideal material since it is a three or four spin system, i.e., two protons per SDA and one or two nearby  $^{29}\text{Si}$  silicon atoms ( $^{29}\text{Si}$  is 4.9% abundant). Proton spin-diffusion should be minimal at a contact time of  $400\ \mu\text{s}$ , especially intermolecular spin-diffusion between SDAs. The  $^{29}\text{Si}$  CPMAS results are in qualitative agreement with the methylene protons of the SDA being in close spatial proximity to the (Si1Al) framework silicons.

**REDOR.** Figure 9 shows the  $^{27}\text{Al}\{^1\text{H}\}$  REDOR curves for several as-made Al-ZSM-12 samples with labeled SDAs. The REDOR curves are consistent with strong dipolar interactions between the protons of the SDA and the aluminum in the zeolite framework, as the REDOR signal decays quickly for all samples. However, the results give no information about which segment of the SDA is closest to the framework aluminum as the REDOR signals' dephasing scale with the number of protons, as might be expected. The strong dephasing of the REDOR signals suggests that the framework aluminum is near the SDA. Also the asymptotic limit of the REDOR fraction  $\Delta S = (S_0 - S)/S_0$  is approximately 0.9 for all samples. Even the  $d_{14}$  sample shows strong dipolar interactions with the framework aluminum as nearly 50% of the aluminum REDOR signal has decayed at an evolution time of 4 ms in the REDOR experiments. As a comparison,  $^{27}\text{Al}\{^1\text{H}\}$  REDOR studies of  $\text{NH}_4^+$ -exchanged mordenite by Blumenfeld and Fripiat<sup>15</sup> show that at an evolution time of 4 ms approximately 80% of the aluminum signal has decayed. They propose a model where the Al–N distance is approximately  $2\ \text{\AA}$ , so for their samples there are four protons that are close to the framework aluminum atoms. As a whole, our  $^{27}\text{Al}$  REDOR experiments suffer due to the strong coupling between the protons and aluminum, i.e., the signal decays quickly for all samples.

The  $^{29}\text{Si}\{^1\text{H}\}$  CP-REDOR curves for the fully protonated Al-ZSM-12 are shown in Figure 10. Both REDOR signals decay quickly although the (Si1Al) signal decays more rapidly. Little can be discerned about the spatial relationship between the SDA and the framework since there are three types of organic protons.  $^{29}\text{Si}\{^1\text{H}\}$  CP-REDOR experiments have also been performed on the  $d_2$ ,  $d_7$ ,  $d_9$ , and  $d_{14}$  samples, though the following discussion will focus on the  $d_7$  and  $d_{14}$  samples since each of these have only one type of organic proton.

The CP-REDOR curves for the  $d_{14}$  sample are shown in Figure 11. This is the most suitable sample for REDOR because (i) the protons are essentially immobile and (ii) there are only

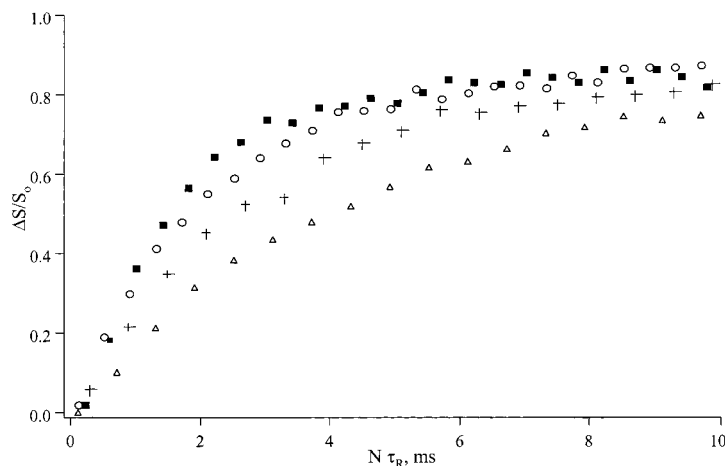


**Figure 9.**  $^{27}\text{Al}\{^1\text{H}\}$  REDOR curves for as-made samples of Al-ZSM-12 with selectively labeled SDAs: (■) fully protonated, (○) benzyl labeled ( $d_7$ ), (+) methyl labeled ( $d_9$ ), and (△) aromatic ring and methyl labeled ( $d_{14}$ ).

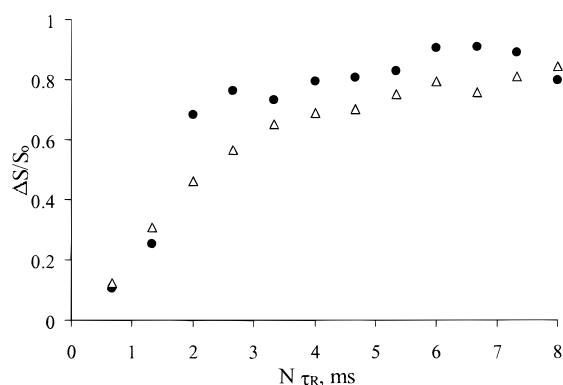


**Figure 10.**  $^{29}\text{Si}\{^1\text{H}\}$  CP-REDOR curves of as-made Al-ZSM-12 synthesized with a fully protonated SDA. Full circles and open triangles correspond to (Si1Al) and (Si0Al) resonances, respectively. A total of 736 scans were acquired per spectrum, and 12 points were acquired. The total acquisition time was 25 h.

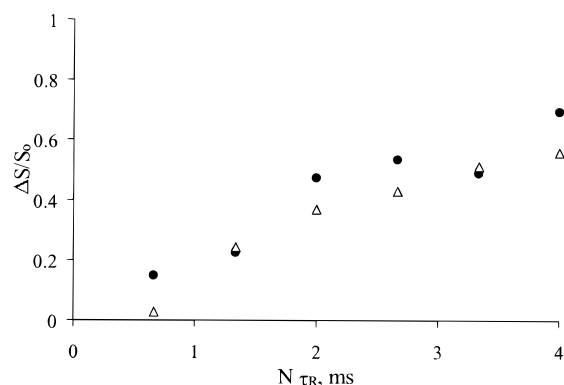


**Figure 12.**  $^{29}\text{Si}\{^1\text{H}\}$  CP-REDOR curves for Al-ZSM-12 made with SDAs labeled at the aromatic ring and methylene positions ( $d_7$ ). Full circles and open triangles correspond to (Si1Al) and (Si0Al) resonances, respectively. A total of 1600 scans were acquired for each spectrum, and six points were acquired. The total acquisition time was 28 h.

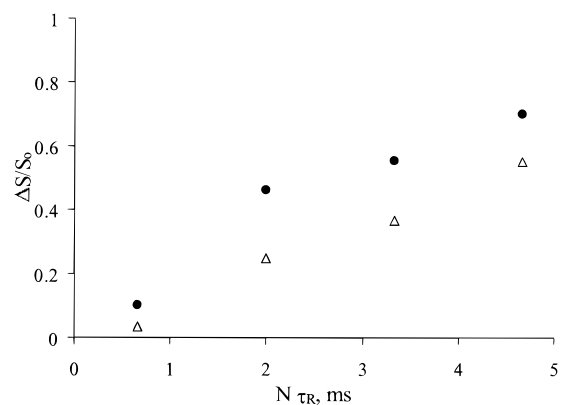


**Figure 11.**  $^{29}\text{Si}\{^1\text{H}\}$  CP-REDOR curves for Al-ZSM-12 made with SDAs labeled at the aromatic ring and methyl position ( $d_{14}$ ). Full circles and open triangles correspond to (Si1Al) and (Si0Al) resonances, respectively. A total of 4256 scans were acquired per spectrum, and four points were acquired. The total acquisition time was approximately 50 h.

two organic protons and one or two  $^{29}\text{Si}$  silicon atoms. The dephasing of both REDOR signals is much slower in this sample as compared to the fully protonated sample. The (Si1Al) signal decays more quickly than the (Si0Al) signal. These results show the methylene protons have stronger dipolar interactions with the (Si1Al) silicons than the (Si0Al) silicons, indicating they are closer to the (Si1Al) silicons. These results are consistent with the  $^{27}\text{Al}\{^1\text{H}\}$  REDOR results for the  $d_{14}$  sample, which

show a dipolar interaction between the methylene protons and the aluminum and are consistent with the interpretation of the  $^{29}\text{Si}$  CPMAS results. Because of the complicated spin dynamics involved in cross-polarization, these results are stronger evidence than the CPMAS experiments. The stronger dipolar interaction of the methylene protons with the (Si1Al) silicons also implies that the nitrogen of the SDA is close to the framework aluminum. The drawback of this sample is the long acquisition times, which preclude obtaining a full REDOR curve (the acquisition of the REDOR curve in Figure 11 took 50 h).

The CP-REDOR curves for the  $d_7$  sample are shown in Figure 12. The (Si0Al) and (Si1Al) REDOR signals decay at approximately the same rate. The CP-REDOR and the CPMAS experiments do not show a preferential dipolar interaction between the methyl protons and the (Si1Al) silicons. This sample is also more complex than the  $d_{14}$  sample for two reasons: (i) the motion of the methyl groups and (ii) their higher number of protons in this sample (nine methyl versus two methylene protons). The results are not conclusive about the methyl protons being preferentially ordered near the (Si1Al) silicons.

## Discussion

The CPMAS and  $^{29}\text{Si}$  REDOR results show that the methylene protons, which are adjacent to the cationic nitrogen, have a stronger dipolar interaction with the (Si1Al) silicons than the (Si0Al) silicons. Because the dipolar interaction is dependent on the internuclear distance ( $\propto r^{-3}$ ), the results indicate the

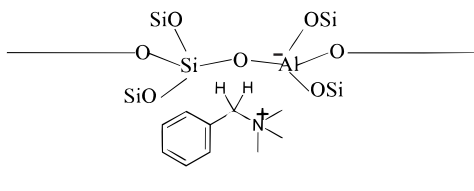


**Figure 13.** Proposed model for as-made Al-ZSM-12 made with benzyltrimethylammonium cations.

methylene protons are preferentially located near the (Si1Al) silicons, which are adjacent to the framework aluminum. The  $^{27}\text{Al}\{^1\text{H}\}$  REDOR results demonstrate there is a strong dipolar coupling between the organic protons and the framework aluminum, which, however, cannot be described in terms of a specific spatial relationship between the SDA and the framework aluminum. Attempts were made to model the  $^{27}\text{Al}\{^1\text{H}\}$  REDOR curve of the  $d_{14}$  sample first by assuming the sample consisted of isolated spin pairs. The data could not be simulated accurately by assuming an isolated spin pair, suggesting that more advanced modeling would be necessary to describe the local structure of the as-made materials. Subsequently, more rigorous simulations were undertaken that explicitly accounted for the presence of three spins (one aluminum, two hydrogens). The simulated REDOR curves were again in poor agreement with the experimental curves. One possible explanation for the discrepancy is due to  $^{27}\text{Al}$  being a quadrupolar nucleus ( $I = 5/2$ ). The nutation behavior of the aluminum causes ambiguity in determining the  $180^\circ$  pulse length, which can lead to incomplete refocusing in the spin echo sequence. Another possible explanation is that the effect of the homonuclear dipolar coupling between the methylene protons is neglected.

On the basis of the NMR results we propose a model for charge ordering in high-silica zeolites. We have shown that the methylene protons of the SDA are closer to the (Si1Al) silicons than the (Si0Al) silicons, which implies they are in close proximity to the framework aluminum. The aromatic protons do not exhibit a selective dipolar interaction with the (Si1Al) silicons, and so we can subsequently conclude they are not spatially located near these silicons. In the case of the methyl protons, the situation is complex due to the multiple rotations of the methyl groups, which will influence both the CPMAS and REDOR behavior and render our results inconclusive. However, the aromatic protons are essentially rigid like the methylene protons and the results show these protons are not in close spatial proximity to the (Si1Al) silicons. Taking these facts into account we propose a model (Figure 13) where the nitrogen of the structure-directing agent is in close proximity to the framework aluminum, and as a result of the SDA's bent geometry, the methyl groups and the aromatic ring are further from the pore wall while the methylene protons are in close proximity to the silicons adjacent to the aluminum.

These results demonstrate the presence of charge ordering in as-made Al-ZSM-12 synthesized with benzyltrimethylammonium cations, which implies that the aluminum has a direct spatial association with the charge center of the SDA. This does not imply that the aluminum could be ordered into discrete crystallographic tetrahedral sites. Thermodynamically, there is little driving force for trivalent atoms to occupy specific T-sites,<sup>16</sup> of which there are seven in the structure of ZSM-12. Also, the SDAs themselves are not ordered in a crystallographic sense.<sup>17</sup> However, the SDAs occluded in the as-made material have a reduced number of possible configurations; in the case of one-dimensional pored materials, the SDAs pack along the length of the pore. We believe these results suggest that the

combination of using SDAs with different charge distributions and a basic knowledge of the SDA's organization in the zeolite micropores should be a useful starting point for a more rational approach to altering the geometric arrangement of framework heteroatoms via synthesis. We are studying this problem using samples of ZSM-12 synthesized with different SDAs but the same framework Si/Al ratio.

## Summary

Samples of Al-ZSM-12 have been prepared using selectively deuterated benzyltrimethylammonium cations where the organic to framework aluminum ratio is approximately 1. The trimethylammonium segment of the SDA undergoes at least two rapid rotations, while the benzyl segment is essentially immobile, undergoing only small wobbling motions. Cross-polarization and rotational echo double resonance NMR experiments have been performed to study the relative orientation and spatial proximity of the SDAs with respect to the zeolite framework. Both CPMAS and REDOR experiments are consistent with the methylene protons of the SDA being spatially located near the silicon atoms adjacent to the framework aluminum. The results are consistent with a model where the framework aluminum is directly associated with the charge center of the SDA. These results demonstrate that it should be possible to alter the spatial arrangement of trivalent atoms in the zeolite framework based on the charge distribution of the SDA used.

**Acknowledgment.** This work was funded from NSF grant CTS-9713516. R.F.L. and D.F.S. acknowledge an NSF International Travel Award to support collaborative work at Westfälische Wilhelms-Universität Münster in the group of H. Eckert (INT-9725941). We thank H. Eckert for use of his laboratory facilities and helpful discussions. We are grateful to the Department of Chemistry and Biochemistry at the University of Delaware for use of the NMR facilities and C. Dybowski for useful discussions.

## References and Notes

- (1) Barrer, R. M. *Hydrothermal Chemistry of Zeolites*; Academic Press: London, 1982.
- (2) (a) Akporiaye, D. E. *Angew. Chem., Int. Ed. Engl.* **1998**, *37*, 2456. (b) Zones, S. I.; Nakagawa, Y.; Lee, G. S.; Chen, C. Y.; Yuen, L. T. *Micropor. Mesopor. Mater.* **1998**, *21*, 199. (c) Yoshikawa, M.; Wagner, P.; Lovall, M.; Tsuji, K.; Takewaki, T.; Chen, C. Y.; Beck, L. W.; Jones, C.; Tzapatsis, M.; Zones, S. I.; Davis, M. E. *J. Phys. Chem. B* **1998**, *102*, 7139. (d) Campbell, B. J.; Bellussi, G.; Carluccio, L.; Perego, G.; Cheetham, A. K.; Cox, D. E.; Millini, R. *Chem. Commun.* **1998**, 1725.
- (3) (a) Lee, Y. J.; Carr, S. W.; Parise, J. B. *Chem. Mater.* **1998**, *10*, 2561. (b) Armor, J. N. *Micropor. Mesopor. Mater.* **1998**, *22*, 451. (c) Geobaldo, F.; Lamberti, C.; Ricchiardi, G.; Bordiga, S.; Zecchina, A.; Palomino, G. T.; Arean, C. O. *J. Phys. Chem.* **1995**, *99*, 11167. (d) Das, S. K.; Dutta, P. K. *Micropor. Mesopor. Mater.* **1998**, *22*, 475. (e) Feuerstein, M.; Lobo, R. F. *Chem. Mater.* **1998**, *10*, 2197.
- (4) (a) Balkus, K. J.; Gabrielov, A. G. *J. Inclusion Phenom. Mol.* **1995**, *21*, 159. (b) Fild, C.; Eckert, H.; Koller, H. *Angew. Chem., Int. Ed. Engl.* **1998**, *37*, 2505. (c) Karge, H. G. *Stud. Surf. Sci. Catal.* **1997**, *105*, 1901. (d) Yan, Y. G.; Vansant, E. F. *J. Phys. Chem.* **1995**, *99*, 14089. (e) Hong, S. B.; Mielczarski, E.; Davis, M. E. *J. Catal.* **1992**, *134*, 349.
- (5) (a) Shantz, D. F.; Lobo, R. F. *J. Phys. Chem. B* **1998**, *102*, 2339. (b) Shantz, D. F.; Lobo, R. F. *Chem. Mater.* **1998**, *10*, 4015.
- (6) (a) Gies, H. *Stud. Surf. Sci. Catal.* **1994**, *85*, 295. (b) Gies, H. *J. Incl. Phenomena* **1986**, *4*, 85. (c) Gies, H. *Z. Kristallogr.* **1986**, *93*, 175. (d) Grünwald-Lüke, A.; Gies, H. *Z. Kristallogr. Suppl.* **1992**, *5*, 88.
- (7) (a) Rosinski, E. J.; Rubin, M. K. U.S. Patent 3,832,449, 1974. (b) Fyfe, C. A.; Gies, H.; Kokotailo, G. T.; Marler, B.; Cox, D. E. *J. Phys. Chem.* **1990**, *94*, 3718.
- (8) (a) Spiess, H. W. *Chem. Rev.* **1991**, *91*, 1321. (b) Vold, R. R. Understanding Chemical Reactivity. In *Nuclear Magnetic Resonance Probes of Molecular Dynamics*; Tycko, R., Ed.; Kluwer: London, 1994; Vol. 8.

(9) (a) Stejskal, E. O. *High-Resolution NMR in the Solid State: Fundamentals of CP/MAS*; Oxford: New York, 1994. (b) Meier, H. In *Advances in Magnetic and Optical Resonance*; Warren, W. S., Ed.; Academic: San Diego, 1994; Vol. 18.

(10) (a) Gullion, T.; Schaefer, J. *J. Magn. Reson.* **1989**, *81*, 196. (b) Gullion, T.; Schaefer, J. In *Advances in Magnetic Resonance*; Warren, W. S. Ed.; Academic: San Diego, 1989; Vol. 13. (c) Fyfe, C. A.; Mueller, K. T.; Grondy, H.; Wong-Moon, K. C. *J. Phys. Chem.* **1993**, *97*, 13484.

(11) Lapod, written by J. Ian Langford, School of Physics and Space Research, University of Birmingham, Birmingham B15 2TT, U.K.

(12) Engelhardt, G.; Michel, D. *High-Resolution Solid State NMR of Silicates and Zeolites*; Wiley: Chichester, U.K., 1987.

(13) Koller, H.; Lobo, R. F.; Burkett, S. L.; Davis, M. E. *J. Phys. Chem.* **1995**, *99*, 12588.

(14) Spiess, H. W.; Sillescu, H. *J. Magn. Reson.* **1981**, *42*, 381.

(15) Blumenfeld, A. L.; Fripiat, J. J. *J. Phys. Chem. B* **1997**, *101*, 6670.

(16) (a) Fripiat, J. G.; Berger-Andre, F.; Andre, J. M.; Derouane, E. G. *Zeolites* **1983**, *3*, 306. (b) Redondo, A.; Hay, J. P. *J. Phys. Chem.* **1993**, *97*, 11754. (c) Ricchiardi, G.; Newsam, J. M. *J. Phys. Chem. B* **1997**, *101*, 9943.

(17) The structure solution of as-made fluoride SSZ-23 is an exception. See: Cambor, M. A.; Díaz-Cabañas M. J.; Perez-Pariente, J.; Teat, S. J.; Clegg, W.; Shannon, I. J.; Lightfoot, P.; Wright, P. A.; Morris, R. E. *Angew. Chem., Int. Ed. Engl.* **1998**, *37*, 2122 for more details.